

Full Length Research Paper

Theoretical studies on nanostructure of 2,6,6-trimethyl-1,3-cyclohexadiene-1-carboxaldehyde

M. Monajjemi^{1*}, F. Naderi², F. Jadidi³ and F. Mollaamin⁴

¹Department of Chemistry, Science and Research Branch, Islamic Azad University, Tehran, Iran.

²Department of basic science, Shahr e Qods branch, Islamic Azad University, Iran.

³Science and Research Branch, Islamic Azad University, Tehran, Iran.

⁴Department of Chemistry, Qom Branch, Islamic Azad University, Qom, Iran.

Accepted 30 June, 2011

The polarized continuum model (PCM) model has been used to optimize 2,6,6-trimethyl-1,3-cyclohexadiene-1-carboxaldehyde (safranal) in aqueous phase, methanol and carbon tetra chloride at B3LYP/6-31G** level of theory and the solvent effect has been studied. The principle of maximum hardness has been tested by calculating chemical hardness and chemical potential at B3LYP/6-31G** level of theory to predict the order of stability of the structure in solutions. The maximum IR intensity is related to the C4=C5 stretching vibrations. Also, the vibrational free energy, heat capacity, entropy, thermal energy and zero point vibrational energy obtained from the calculated frequencies and these are compared in different media.

Key words: Polarized continuum model (PCM), functional theory methods (DFT), solvent, IR, safranal.

INTRODUCTION

The biological activity of saffron as a natural preventing substance in anticancer research is in development (Mollaamina et al., 2011; Mollaamin et al., 2010; Abe and Saito, 2000; Soeda et al., 2001; Monajjemi et al., 2009; Abdullaev et al., 2002; Abdullaev et al., 2003; Rivero'n-Negrete et al., 2002). Saffron is the world's most expensive spice and apart from its traditional value as food additive recent studies indicate its potential as an anti-cancer agent.

The value of saffron (dried stigmas of *Crocus sativus* L.) is determined by the existence of three main secondary metabolites: crocin and its derivatives which are responsible for color; picrocrocin, responsible for taste; and safranal responsible for odor. The amount of these compounds in dried stigma tissues is the most important indicator of quality of this spice.

Safranal, a pleasantly odoriferous component of saffron develops during the process of drying by hydrolysis of the bitter substance picrocrocin, which is present in the fresh stigmata. The Greeks considered saffron as a sensual perfume. It was strewn in Greek halls, courts, theatres and in Roman baths. In Rome the streets were sprinkled

with saffron when Nero entered the city. In the Middle East saffron is used to prepare an oil-based perfume called 'Zaafiran Attar', which is a mixture of saffron and sandalwood.

An alcoholic tincture of saffron is sometimes used as a fragrance ingredient particularly in oriental-type perfumes. Saffron is used as a perfume ingredient in many famous perfume brands. The spices is also employed in some types of incense. Nowadays the use of saffron in the cosmetic industry is increasing owing to its active substances and to the trend to use natural products in cosmetic formulations (Basker and Negbi, 1983; Safinter, 1999; [www. Babysaffron.com/gis. html](http://www.Babysaffron.com/gis.html)).

Safranal is the main component of the essential oil and is responsible for the characteristic saffron aroma, which is obtained from picrocrocin and 4-hydroxy-2,6,6-trimethyl-1-cyclohexene-1-carboxaldehyde (HTCC) during the saffron drying process (Iborra et al., 1992; Raina et al., 1996; Himeno and Sano, 1987; Lozanoa et al., 2000). As this compound is not present in the fresh stigma, its concentration in saffron depends strongly on both the drying and storage conditions.

Safranal, the principal substance responsible for the aroma of saffron, has the molecular formula C₁₀H₁₄O, which corresponds to 2,6,6-trimethyl-1,3-cyclohexadiene-1-carboxaldehyde (Gonzalo et al., 1996).

*Corresponding author. E-mail: m_monajjemi@yahoo.com.

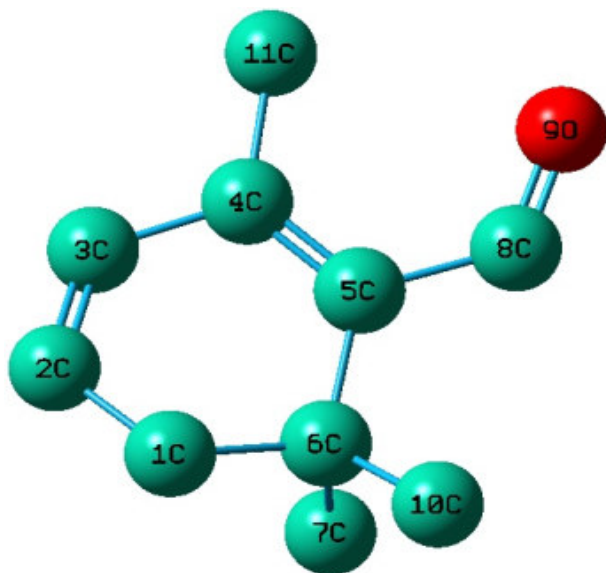


Figure 1. Numbering system adopted in this study (Safranal) (without H).

METHODOLOGY

In the present study, *ab initio* Hartree-Fock (HF) theory and density functional theory methods (DFT) have been used to optimize the geometries of safranal. The Becke's three parameter exact exchange functional (B3) (Monajjemi et al., 2010) combined with gradient corrected correlation functional of Lee–Yang–Parr (LYP) [18] and BLYP of DFT methods have been employed to optimize the molecules by implementing the 6-31G,6-31G*,6-31G basis sets. We found 6-31G** is the best basis set.

The effects of the media on the molecular geometry of safranal with the solvents of water (78.39), Methanol (32.63), Carbon tetrachloride (2.228) at 293.15, 298.15, 303.15, 305.15, 308.15, 310.15 and 315.15 K were investigated by the PCM theory.

The solute–solvent interaction studies have been performed using the self-consistent reaction field theory (SCRf) (Wong et al., 1991) at B3LYP/6-31G** level of theory. This method is based on Tomasi's polarized continuum model (PCM), which defines the cavity as the union of a series of interlocking atomic spheres. Vibration frequency analyses have been carried out using the analytical second derivatives at B3LYP/6-31G** level of theory in gaseous and solvent phases to determine the nature of a stationary point obtained through geometry optimization process. All the calculations have been performed using GAUSSIAN98W computational package (Frisch et al., 2001).

The chemical hardness (η) have been determined for all the safranal using the highest occupied molecular orbital (HOMO) and lowest unoccupied molecular orbital (LUMO) energies at B3LYP /6-31G (2d, 2p) level of theory. Quantum chemistry descriptors include: energy of the highest occupied molecular orbital (E_{HOMO}), energy of the lowest unoccupied molecular orbital (E_{LUMO}), hardness (η), electronegativity (χ), softness (S) and electrophilicity index (ω).

RESULTS AND DISCUSSION

The labeling of atoms in 2,6,6-trimethyl-1,3-cyclohexadiene-1-carboxaldehyde is given in Figure 1.

The optimized geometrical parameters (bond length, order and angle) in gas phase are listed in Table 1. The dipole of a molecule induced a dipole in the medium, and the electric field of the solvent dipole in turn interacts with the molecular dipole, leading to a overall stabilization (Monajjemi et al., 2011).

Comparing the values calculated at the B3LYP/6-31G** level with the result at the HF/6-31G** level, we found that the C=C bond length increases by more than 0.021Å°, the C=O bond length increases 0.031Å°, while changes in the C4–C11, C6–C7, C6–C10 bond lengths are less than 0.006Å°. From previous studies it is known that the DFT methods can achieve greater accuracy than the Hartree–Fock theory (Foresman and Frisch, 1996; Wiest et al., 1994).

Solvent effects are important in molecular thermodynamic properties, including zero-point vibrational energy (ZPVE), enthalpy, free energy and total energy.

ZPVE is needed for theoretical studies of thermochemistry. The ZPVE in the gas phase is 135.41078 (kcal/mol). Comparing the gas phase, time ZPVE increases to 135.494 (kcal/mol) in CCl₄, 135.499 (kcal/mol) in methanol and 135.523 (kcal/mol) in the water. Sum of electronic and thermal Enthalpies in the gas phase is -464.478082 kcal/mol. Comparatively, this parameter in CCl₄, methanol and in water, decreases 0.0001, 0.0001 and 0.0002 kcal/mol, respectively. Sum of electronic and thermal Free Energies of the gas phase is -464.52672 kcal/mol. For the CCl₄, methanol and water, this parameter decreases 0.0002, 0.0007 and 0.0008 kcal/mol, respectively.

The total energy in the gas phase is 464.70621 kcal/mol. In comparison with the gas phase, the total energies in the CCl₄, methanol and water become much lower, decrease 0.00018, 0.011 and 0.0062 kcal/mol, respectively. Hence, the molecule in solvent is more stable than the neutral. In addition, the corresponding dipole moments increase in going from the gas phase to solutions, 0.44 (CCl₄), 1.69 (methanol) and 1.75 (water) Debye, respectively. Therefore, the molecular polarity in medium is little stronger than that in the neutral.

The DFT calculated frequencies in the solvents were obtained using the PCM model at the B3LYP/6-31G** level. The calculated frequencies and their intensities are given in Table 3. The safranal (Figure 1) belongs to C₁ point group and 69 normal mode vibrational frequencies. The shifts of frequencies and changes of IR intensities from the gas phase to medium are listed in Table 2. On going from the gas phase to solutions, shifts of frequencies are nearly same in Carbon tetra chloride and gas phase. In the methanol and water, there is small frequency shifts for u1, u4- u11, u 14, u17- u 30, u 32- u 35, u 37- u 40, u 44, u 53, u 54, u 56- u 64, u 66 and u 67. For instance, significant changes of IR intensities are observed in u36, u 55, u 65, u 68 and u 69. Where, u36 is Methyl antisymmetric stretching and C–H stretching vibration has the largest changes in intensities (up to 97 km.mol⁻¹ in the CCl₄). Spectrums that have the highest

Table 1. Optimized geometry for Safranal in gas phase.

Coordinate a	6-31G**					
	B3LYP		BLYP		HF	
	Length/ Angle	order	Length/ Angle	order	Length/ Angle	order
C(1)-C(2)	1.499	1	1.508	1	1.501	1
C(1)-C(6)	1.549		1.562		1.541	
C(1)-H(12)	1.097		1.104		1.086	
C(1)-H(13)	1.103		1.111		1.091	
C(2)-C(3)	1.343		1.355		1.322	
C(2)-H(14)	1.087		1.094		1.077	
C(3)-C(4)	1.464		1.468		1.478	
C(3)-H(15)	1.087		1.094		1.076	
C(4)-C(5)	1.371		1.387		1.342	
C(4)-C(11)	1.509		1.519		1.509	
C(5)-C(6)	1.545		1.558		1.541	
C(5)-C(8)	1.470		1.477		1.484	
C(6)-C(7)	1.547		1.560		1.541	
C(6)-C(10)	1.546		1.558		1.542	
C(7)-H(16)	1.094		1.101		1.084	
C(7)-H(17)	1.097		1.104		1.087	
C(7)-H(18)	1.095		1.102		1.086	
C(8)-O(9)	1.226		1.241		1.195	
C(8)-H(19)	1.109		1.118		1.094	
C(10)-H(20)	1.093		1.100		1.084	
C(10)-H(21)	1.096		1.103		1.086	
C(10)-H(22)	1.095		1.102		1.086	
C(11)-H(23)	1.095		1.102		1.087	
C(11)-H(24)	1.094		1.101		1.086	
C(11)-H(25)	1.093		1.100		1.076	
C(2)-C(1)-C(6)	113.464		113.615		113.224	
C(2)-C(1)-H(12)	110.791		110.825		110.503	
C(2)-C(1)-H(13)	108.090		108.057		108.042	
C(6)-C(1)-H(12)	109.057		109.075		109.132	
C(6)-C(1)-H(13)	109.392		109.387		109.441	
H(12)-C(1)-H(13)	105.751		105.559		106.255	
C(1)-C(2)-C(3)	120.217		120.211		120.385	
C(1)-C(2)-H(14)	119.108		119.094		118.897	
C(3)-C(2)-H(14)	120.584		120.590		120.662	
C(2)-C(3)-C(4)	121.807		122.025		121.563	
C(2)-C(3)-H(15)	120.587		120.453		120.835	
C(4)-C(3)-H(15)	117.562		117.476		117.574	
C(3)-C(4)-C(5)	119.589		119.726		119.505	
C(3)-C(4)-C(11)	116.319		116.396		114.362	
C(5)-C(4)-C(11)	124.089		123.874		126.127	
C(4)-C(5)-C(6)	120.626		120.424		121.146	
C(4)-C(5)-C(8)	120.885		121.030		121.824	
C(6)-C(5)-C(8)	118.088	1	118.136	1	116.702	1
C(1)-C(6)-C(5)	109.863	1	110.027	1	109.656	1
C(1)-C(6)-C(7)	109.793	1	109.738	1	109.912	1
C(1)-C(6)-C(10)	106.863	2	106.833	2	106.846	2
C(5)-C(6)-C(7)	108.418	1	108.277	1	109.186	1
C(5)-C(6)-C(10)	112.897	1	112.961	1	112.147	1
C(7)-C(6)-C(10)	108.978	1	108.975	1	109.058	1

Table 1. Contd

C(6)-C(7)-H(16)	111.174	2	111.244	2	111.158	2
C(6)-C(7)-H(17)	110.704	1	110.675	1	110.709	1
C(6)-C(7)-H(18)	110.847	1	110.852	1	111.116	1
H(16)-C(7)-H(17)	108.231	1	108.175	1	108.276	1
H(16)-C(7)-H(18)	107.965	1	107.954	1	107.850	1
H(17)-C(7)-H(18)	107.793	1	107.811	1	107.591	1
C(5)-C(8)-O(9)	126.349	1	126.482	1	126.553	1
C(5)-C(8)-H(19)	114.894	1	114.746	1	114.692	1
O(9)-C(8)-H(19)	118.753	1	118.768	1	118.755	1
C(6)-C(10)-H(20)	112.888	2	112.865	2	112.869	2
C(6)-C(10)-H(21)	109.494	1	109.515	1	109.669	1
C(6)-C(10)-H(22)	111.408	1	111.403	1	111.284	1
H(20)-C(10)-H(21)	106.931	1	106.990	1	106.896	1
H(20)-C(10)-H(22)	108.097	1	108.048	1	108.104	1
H(21)-C(10)-H(22)	107.803	1	107.803	1	107.801	1
C(4)-C(11)-H(23)	110.983	1	111.063	1	109.439	1
C(4)-C(11)-H(24)	110.476	1	110.542	1	109.409	1
C(4)-C(11)-H(25)	111.857		111.845		113.385	
H(23)-C(11)-H(24)	108.495		108.495		107.122	
H(23)-C(11)-H(25)	105.216		104.960		107.721	
H(24)-C(11)-H(25)	109.640		109.750		109.564	

Table 2. The calculated frequencies and their intensities.

No.	Gas phase		Carbon tetrachloride			Methanol			Water		
	freq. ^a	Int.(IR)	freq. ^a	Δ^b	Int.(IR)	freq. ^a	Δ^b	Int.(IR)	freq. ^a	Δ^b	Int.(IR)
u1	65.624	1.1	65.444	-0.18	0.79	72.754	7.13	0.39	71.526	5.90	0.38
u2	95.871	1.2	97.786	1.915	1.47	115.51	19.64	1.06	115.341	19.5	1.04
u3	132.644	0.26	131.084	-1.56	0.26	134.63	1.986	0.29	133.989	1.35	0.3
u4	164.694	2.46	166.979	2.285	2.19	172.345	7.651	1.96	172.628	7.94	1.84
u5	214.397	5.24	214.783	0.386	5.71	222.516	8.119	6.95	222.443	8.05	7.04
u6	235.491	1.14	237.104	1.613	1.08	243.927	8.436	1.21	243.971	8.48	1.25
u7	279.282	2.02	281.063	1.781	2.19	286.52	7.238	2.35	286.574	7.30	2.4
u8	295.395	1.31	297.094	1.699	0.94	305.973	10.578	0.15	306.488	11.1	0.11
u9	308.009	0.58	309.146	1.137	0.68	313.013	5.004	0.97	313.178	5.17	0.99
u10	326.487	1.59	327.04	0.553	1.52	328.507	2.02	1.64	328.571	2.09	1.61
u11	335.72	0.52	337.056	1.336	0.57	341.665	5.945	0.36	342.045	6.33	0.36
u12	366.734	0.55	366.478	-0.256	0.59	369.362	2.628	0.49	369.17	2.44	0.48
u13	407.357	2.06	408.295	0.938	2.22	409.135	1.778	2.4	409.243	1.89	2.44
u14	442.409	1.05	443.214	0.805	0.95	445.789	3.38	0.91	445.956	3.58	0.9
u15	480.504	2.65	480.862	0.358	2.6	482.288	1.784	2.46	482.477	1.98	2.45
u16	502.216	6.83	502.589	0.373	6.79	504.088	1.872	6.76	504.173	1.96	6.76
u17	566.954	0.59	568.861	1.907	0.7	569.482	2.528	0.79	570.116	3.16	0.83
u18	629.99	5.27	630.539	0.549	5.19	634.203	4.213	4.99	634.296	4.31	4.95
u19	685.296	20.58	687.104	1.808	20.56	689.378	4.082	20.18	689.826	4.53	20.2
u20	751.262	22.28	751.958	0.696	22.39	756.394	5.132	22.52	756.575	5.31	22.6
u21	807.533	6.94	810.497	2.964	6.63	813.151	5.618	5.8	813.877	6.34	5.82
u22	846.773	4.19	848.924	2.151	3.96	850.511	3.738	4.21	851.137	4.36	4.12
u23	908.918	1.36	910.952	2.034	1.38	912.55	3.632	1.23	913.121	4.20	1.25
u24	931.819	2.78	934.51	2.691	2.43	935.658	3.839	2.34	936.574	4.75	2.24
u25	947.801	0.26	949.737	1.936	0.25	952.333	4.532	0.26	953.054	5.25	0.27

Table 2. Contd.

u26	990.213	0.88	990.764	0.551	0.51	994.229	4.016	1.44	994.41	4.19	1.07
u27	992.357	4.17	993.976	1.619	4.35	995.874	3.517	3.11	996.365	4.01	3.55
u28	1009.58	1.78	1009.63	0.048	1.91	1011.84	2.254	2.03	1011.94	2.36	2.03
u29	1022.26	6.43	1024.096	1.834	6.43	1025.85	3.584	6.66	1026.33	4.07	6.61
u30	1038.60	0.4	1039.633	1.035	0.43	1042.03	3.436	0.39	1042.41	3.82	0.4
u31	1056.31	5.28	1056.811	0.501	5.29	1058.46	2.148	5.56	1058.51	2.19	5.39
u32	1071.16	3.67	1073.847	2.685	3.75	1073.55	2.391	3.89	1074.61	3.45	3.93
u33	1135.56	36.48	1138.557	2.997	32.94	1141.97	6.409	26.61	1142.60	7.03	26.85
u34	1167.06	27.03	1171.363	4.305	27.31	1176.42	9.365	27.56	1177.04	9.99	27.39
u35	1200.8	8.24	1203.084	2.284	9.28	1205.12	4.317	10.11	1205.79	4.98	10.3
u36	1221.82	14.88	1124.731	-97.087	15.73	1225.96	4.14	15.74	1126.99	-94.8	15.97
u37	1234.81	3.7	1237.099	2.293	3.5	1238.47	3.663	5.04	1239.10	4.29	4.8
u38	1269.90	4.92	1271.421	1.523	5.06	1273.33	3.427	5.41	1273.79	3.89	5.38
u39	1313.53	14.37	1316.552	3.019	14.27	1317.64	4.103	13.62	1318.66	5.13	13.6
u40	1367.15	2.78	1368.743	1.587	2.8	1370.78	3.622	2.8	1371.05	3.89	2.82
u41	1409.72	6.5	1411.767	2.047	6.6	1411.85	2.13	6.73	1412.34	2.62	6.77
u42	1420.15	17.57	1421.144	0.991	17.93	1421.82	1.667	18.24	1421.971	1.82	18.38
u43	1430.86	8.17	1432.618	1.761	8.31	1432.61	1.757	8.65	1432.98	2.13	8.86
u44	1440.96	0.96	1442.736	1.773	1.09	1444.61	3.646	1.4	1445.00	4.04	1.45
u45	1463.30	8.91	1464.035	0.731	8.72	1462.35	-0.956	7.97	1462.39	-0.91	7.95
u46	1474.9	3.37	1474.869	-0.031	3.44	1475.38	0.477	3.46	1475.31	0.40	3.45
u47	1484.94	9.25	1485.428	0.49	9.61	1486.07	1.131	10.87	1486.05	1.12	10.48
u48	1489.73	4.44	1490.075	0.344	4.29	1490.65	0.915	5.82	1490.82	1.10	5.46
u49	1499.34	0.23	1499.647	0.308	0.25	1500.15	0.815	0.31	1500.22	0.88	0.31
u50	1505.77	6.17	1506.422	0.645	6.24	1506.61	0.834	6.28	1506.74	0.96	6.28
u51	1522.67	5.75	1523.314	0.643	5.99	1523.93	1.26	7.31	1524.12	1.44	7.29
u52	1525.95	4.04	1526.57	0.623	4.15	1526.39	0.45	5.16	1526.54	0.59	5.25
u53	1582.44	182.97	1583.239	0.8	189.34	1574.41	-8.03	202.47	1575.22	-7.2	203.89
u54	1698.02	6.47	1698.286	0.268	6.79	1689.60	-8.42	10.95	1689.63	-8.4	11.63
u55	1756.86	172.3	1749.716	-7.146	167.54	1721.47	-35.4	151.07	1721.05	-35.8	148.52
u56	2934.36	125.98	2939.435	5.072	124.47	2940.93	6.57	120.63	2941.08	6.72	120.42
u57	2985.40	26.82	2985.459	0.06	26.84	2974.56	-10.8	26.76	2975.63	-9.8	26.75
u58	3034.65	22.6	3033.904	-0.75	22.79	3028.84	-5.81	22.69	3028.72	-5.9	22.78
u59	3044.24	28.1	3043.53	-0.715	28.89	3039.54	-4.71	27.03	3039.52	-4.7	27.27
u60	3053.47	17.18	3052.683	-0.785	16.86	3048.16	-5.31	14.95	3048.39	-5.1	14.87
u61	3062.05	24.14	3063.526	1.47	23.42	3053.28	-8.78	23.76	3054.33	-7.7	23.38
u62	3103.63	13.64	3101.925	-1.705	13.33	3097.60	-6.02	15.95	3097.43	-6.02	16.11
u63	3109.85	38.41	3108.345	-1.509	39.19	3106.28	-3.58	36.89	3106.28	-3.6	37.06
u64	3116.92	11.42	3115.211	-1.707	11.8	3108.97	-7.94	12.71	3109.04	-7.9	12.72
u65	3124.71	13.6	3123.085	-1.622	13.56	3114.47	-10.2	15.52	3113.91	-10.8	15.56
u66	3128.72	30.07	3126.807	-1.912	30.34	3121.00	-7.7	28.5	3120.80	-7.9	28.43
u67	3137.19	12.74	3135.989	-1.199	12.84	3132.99	-4.2	13.18	3133.05	-4.1	13.53
u68	3169.79	4.55	3169.525	-0.265	4.52	3156.43	-13.3	4.67	3156.25	-13.5	4.73
u69	3190.87	31.86	3190.449	-0.421	31.87	3179.16	-11.7	31.96	3178.96	-11.9	32.04

(a) PCM Model at the B3LYP/6-31G** level.

(b) Shifts of frequencies and changes of IR intensities from the gas phase to solutions.

intensity of IR are u 53, u 55 and u 56; where maximum IR intensity is in u 53 (in water: freq=1575.22 cm⁻¹ and intensity=203.895 km mol⁻¹).

It is related to the C4=C5 stretching vibrations. This frequency difference between water and gas phase is

to -7.22. IR spectrum intensity increases with increasing dielectric constant from gas toward the water. u 55 (in water: freq=1721.05 cm⁻¹ and IR intensity=148.52 km.mol⁻¹) is related to the mixed modes of C8=O9 and C4=C5 stretching vibrations. u 56 (in water: freq=2941.09

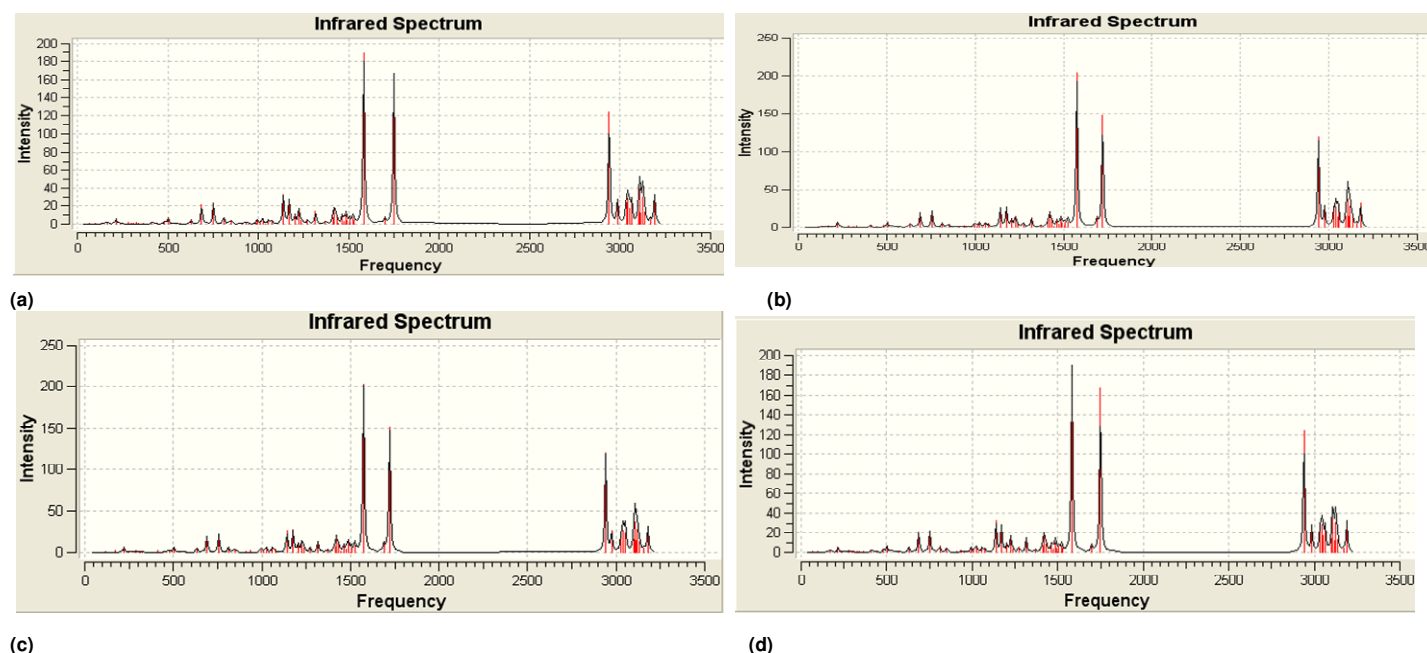


Figure 2. The calculated IR spectra in gas phase and solutions. (a) Gas phase (b) Water (c) Methanol (d) Carbon tetrachloride.

Table 3. Thermodynamic properties at different temperatures at B3LYP/6-31G** level.

Temp. (K)	Carbon tetrachloride			Methanol			Water		
	Cv ^a	S ^b	E(Thermal) ^c	Cv ^a	S ^b	E(Thermal) ^c	Cv ^a	S ^b	E(Thermal) ^c
293.05	43.056	101.460	142.403	42.882	100.520	142.327	42.866	100.548	142.350
298.15	43.735	102.251	142.627	43.564	101.308	142.550	43.547	101.335	142.573
303.15	44.375	102.994	142.841	44.206	102.048	142.763	44.189	102.075	142.786
308.15	45.034	103.758	143.064	44.868	102.809	142.985	44.851	102.836	143.008
310.15	45.298	104.063	143.154	45.132	103.113	143.075	45.115	103.140	143.098
313.15	45.693	104.521	143.291	45.529	103.569	143.211	45.512	103.596	143.234

(a) cal.mol⁻¹K⁻¹ (b) cal.mol⁻¹K⁻¹ (c) kcal.mol⁻¹

cm⁻¹ and IR intensity=120.42 km.mol⁻¹) is related to the C8-H19 stretching vibrations. The calculated IR spectra in gas phase and solutions in Figures 2 and 3 show the IR spectrum intensity diagram according to dielectric constant in ϵ 53.

On the basis of vibrational analyses and statistical thermodynamics, the standard thermodynamic functions: heat capacity (Cv), entropy (S) and thermal energy (E) were obtained and listed in Table 3. As observed from Figure 3 and Figure 4, all the values of Cv, S and E increase with the increase of temperature from 290.15 to 313.15, which is attributed to the enhancement of the molecular vibration while the temperature increases. The chemical hardness (η) and chemical potential (μ) are important tools to study the relative stabilities of a molecule. The chemical hardness parameter received much attention after the invention of Pearson's maximum hardness principle (Pearson, 1973), which states that the minimum energy structure has the maximum chemical

hardness. The chemical hardness and chemical potentials of safranal are calculated at B3LYP/6-31G ** level of theory for both gaseous and solution phases. The maximum hardness principle (MHP) is able to predict the most stable structure. As you see in Table 4 the calculated chemical hardness values in solution phase are more or less similar to that of gas phase and indicate that there is no considerable change in molecular orbital energies of the structure in SCRF calculations.

Conclusion

Density-functional calculations were performed to determine electric and thermo chemical properties of safranal (the main component of the essential oil and is responsible for the characteristic saffron aroma). On going from the gas phase to solutions and, the solvent reaction field has general weak influence on the skeletal

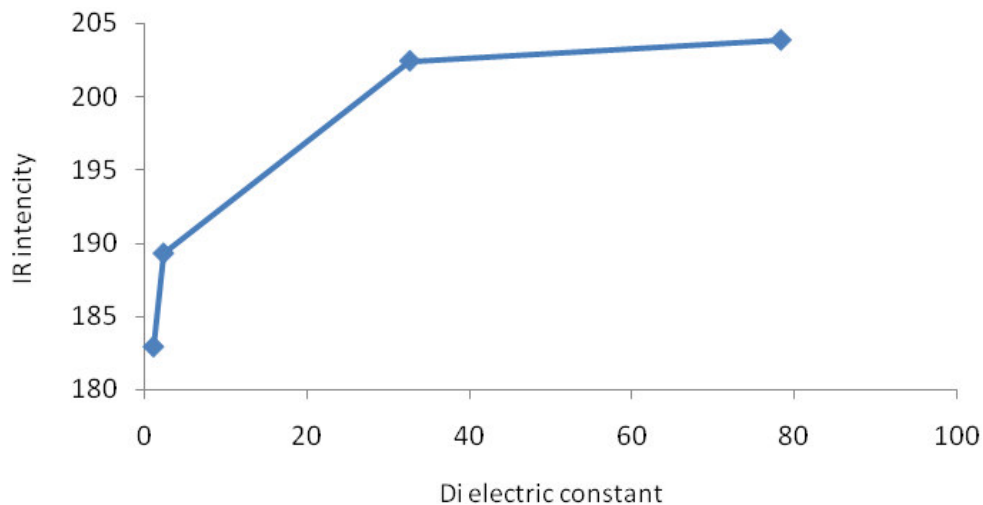


Figure 3. IR spectrum intensity versus dielectric constant from gas toward the water in ν_{53} .

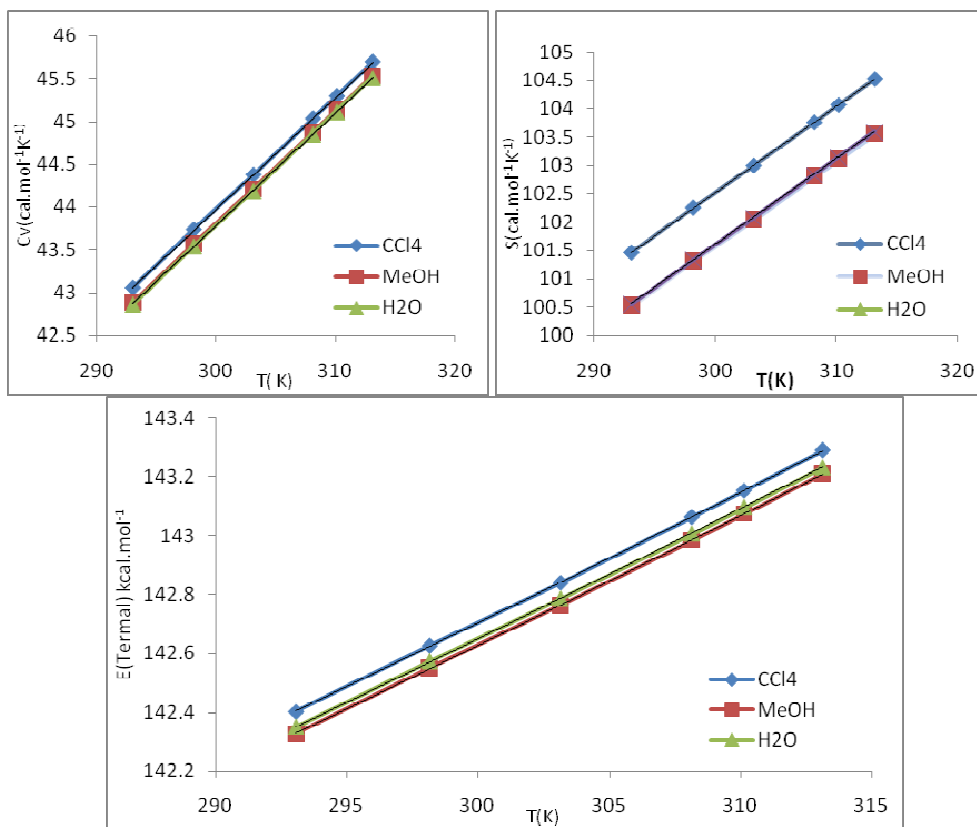


Figure 4. C_v , S and E versus T for the title compound.

Table 4. η , χ , S , ω in gas phase and CCl_4 , MeOH and H_2O .

Medium	η	χ	S	ω
Phase Gas	0.0769	-0.0769	6.5019	0.0383
Tetrachloride carbon	0.0763	-0.0763	6.5530	0.0380
Methanol	0.0746	-0.0746	6.7024	0.0368
Water	0.0745	-0.07455	6.7069	0.0368

bond angles, dipole moment, and thermodynamics properties of the molecule. The frequencies using the PCM model at the B3LYP/6-31G** level were calculated. The infrared spectrum of the molecule is weak influenced by the solvent reaction field. ν_{36} is Methyl antisymmetric stretching and C–H stretching vibration has the largest changes in intensities (up to 97 km.mol^{-1} in the CCl_4). Spectrums that have the highest intensity of IR are ν_{53} , ν_{55} and ν_{56} . All the values of C_v , S and E increase with the increase of temperature from 290.15 to 313.15. The calculated chemical hardness values in solution phase are more or less similar to that of gas phase and indicate that there is no considerable change in molecular orbital energies of the structure in SCRF calculations.

REFERENCES

- Abdullaev FI, Rivero'n-Negrete L, Caballero-Ortega H, Manuel Herna'ndez J, Pe'rez-Lo'pez I, Pereda-Miranda R, Espinosa-Aguirre JJ (2003). Use of *in vitro* assays to assess the potential antigenotoxic and cytotoxic effects of saffron (*Crocus sativus* L.). *Toxicol. In Vitro*, *17*: 731-736.
- Abdullaev FJ, Caballero-Ortega H, Rivero'n-Negrete L, Pereda-Miranda R, Rivera-Luna R, Manuel Herna'ndez J, Pe'rez-Lo'pez I, Espinosa-Aguirre JJ (2002). *In vitro* evaluation of the chemopreventive potential of saffron., *Rev. Invest. Clin.*, *54*: 430- 436.
- Abe K, Saito H (2000). Effects of saffron extract and its constituent crocin on learning behaviour and long-term potentiation. *Phytother. Res.*, *14*: 149-152.
- Basker D, Negbi M (1983). Uses of Saffron, *Econ. Bot.*, *37*: 228–236.
- Frisch MJ, Trucks GW, Schlegel HB, Scuseria GE, Robb MA, Cheeseman JR, Zakrzewski VG, Montgomery JA, Stratmann RE, Burant JC, Dapprich S, Millam JM, Daniels AD, Kudin KN, Strain MC, Farkas O, Tomasi J, Barone V, Cossi M, Cammi R, Mennucci B, Pomelli C, Adamo C, Clifford S, Ochterski J, Petersson GA, Ayala PY, Cui Q, Morokuma K, Rega N, Salvador P, Dannenberg JJ, Malick DK, Rabuck AD, Raghavachari K, Foresman JB, Cioslowski J, Ortiz JV, Baboul AG, Stefanov BB, Liu G, Liashenko A, Piskorz P, Komaromi I, Gomperts R, Martin RL, Fox DJ, Keith T, Al-Laham MA, Peng CY, Nanayakkara A, Challacombe M, Gill PMW, Johnson B, Chen W, Wong MW, Andres JL, Gonzalez C, Head-Gordon M, Replogle ES, Pople JA (2001.) GAUSSIAN98, Revision A.11.2, Gaussian, Inc., Pittsburgh, PA, 2001.
- Himeno H, Sano K (1987). Synthesis of Crocin, Picrocrocine and Safranal by Saffron Stigma-like Structures Proliferated *in vitro*, *Agric. Biol. Chem.*, *51*: 2395-2400.
- Iborra JL, Castellar MR, Ca'novas M, Manjo'n A (1992). TLC Preparative Purification of Picrocrocine, HTCC and Crocin from Saffron. *J. Food Sci.*, *57*: 714-716.
- Lozanoa P, Delgadob D, Go'mezb D, Rubiob M, Iborra JL (2000). A non-destructive method to determine the safranal content of saffron (*Crocus sativus* L.) by supercritical carbon dioxide extraction combined with high-performance liquid chromatography and gas chromatography, *J. Biochem. Biophys. Methods*, *43*: 367-378.
- Mollaamin F, Layali I, Ilkhani AR, Monajjemi M (2010). Nanomolecular simulation of the voltage-gated potassium channel protein by gyration radius study. *Afr. J. Microbiol. Res.*, *4*: 2795-2803.
- Mollaamina F, Varmaghani Z, Monajjemi M (2011). Dielectric effect on thermodynamic properties in vinblastine by DFT/Onsager modeling, *Phy. Chem. Liq.*, *49*: 318-336.
- Monajjemi M, Honarparvar B, Nasser SM, Khaleghian M (2009). NQR and NMR study of hydrogen bonding interactions in anhydrous and monohydrated guanine cluster model: A computational study *Journal of Structural Chemistry, J. Struct. Chem.*, *50*: 67-77.
- Monajjemi M, Razavian MH, Mollaamin F, Naderi N, Honarparvar B (2008). A Theoretical thermochemical study of solute-solvent dielectric effects in the displacement of codon-anticodon base pairs, *J. Russian Phys. Chem. A.*, *82*: 113-121.
- Pearson RG (1973). *Hard and Soft Acids and Bases*, Dowden (Hutchinson & Ross), Stroudsburg, PA.
- Raina BL, Agarwal SG, Bhatia AK, Gaur GS (1996). Changes in Pigments and Volatiles of Saffron (*Crocus sativus*L) During Processing and Storage. *J. Sci. Food Agric.*, *71*: 27-32.
- Rivero'n-Negrete L, Caballero-Salazar S, Ordaz-Tellez M, G, Abdullaev F (2002). The combination of natural and synthetic agents a new pharmacological approach in cancer chemoprevention. *Proc. West Pharmacol.*, *45*: 74-75.
- Soeda S, Ochiai T, Paopong L, Tanaka H, Shoyama Y, Shimeno H (2001). Crocin suppresses tumor necrosis factor- α -induced cell death of neuronally differentiated PC-12 cells, *Life Sci.*, *69*: 2887-2898.
- Wiest O, Black KA, Houk KN (1994). Density Functional Theory Isotope Effects and Activation Energies for the Cope and Claisen Rearrangements, *J. Am. Chem. Soc.*, *116*: 10336–10337.